Design and Analysis of Reconfigurable MIMO Antennas for 5G Wireless Networks

Dr. A V Prabhu[1], Dr.M.Arulkumar[2]

[1]Associate Professor, Department of ECE,
Koneru Lakshmaiah Education Foundation, Vijayawada, Andhra Pradesh, India.
[2]Assistant Professor (Sr.Grade), Department of ECE,
Government College of Engineering, Bargur-635104, Tamilnadu, India.

Article Info	ABSTRACT
	The introduction of 5G systems means a sharp increase in the need for antennas supporting ultra-high rates, quick responses and flexible spectrum use, mainly in the millimeter-wave (mmWave) area. This paper details the creation, modeling and evaluation of a Multiple-Input Multiple-Output (MIMO) antenna system for use in 5G mmWave bands. The system uses varactor diodes, RF Micro-Electro-Mechanical Systems (MEMS) switches and Defected Ground Structures (DGS) to make it reconfigurable in both radiation direction and operating frequency. Because of these elements, the system can turn beams regularly and quickly switch frequencies over the 24–30 GHz band for 5G NR bands n257 and n258. The compact Rogers RT/Duroid 5880 was chosen for the design of the antenna array and CST Microwave Studio was used to optimize it for high isolation (>25 dB), low ECC (<0.02) and high radiation efficiency (>85%). Thorough parametric analysis was used to check how performance metrics such as gain, beam overview and coupling decrease due to different reconfiguration mechanisms. Simulation results are confirmed by tests of the prototype which demonstrate that the system can re-tune frequencies, beam in a specific direction (+/- 30°) and always works well in MIMO mode. Because Channel Capacity Loss (CCL) is below 0.3 bps/Hz and Diversity Gain (DG) is above 9.9 dB, the diversity performance is ideal for situations with many users and lots of pathways. The antenna, as described, gives more choices along with a compact design, together with meeting all the requirements expected by next-generation wireless, vehicular and adaptive 5G base station systems. The scalable and low-power benefits of its hybrid approach mean it is a big step forward in the design of 5G and future wireless network antennas.

Corresponding Author:

Dr. A V Prabhu,
Associate Professor, Department of ECE,
Koneru Lakshmaiah Education Foundation, Vijayawada, Andhra Pradesh, India.

1. INTRODUCTION

Mobile communication in the fifth generation (5G) requires handling much more data fast, using the airwaves more efficiently, decreasing the time delay between actions by users and

connecting mobile devices across various kinds of surroundings [6]. To reach these ambitious targets, 5G is being built using higher frequency bands, mainly in the 24 GHz to 40 GHz millimeter-wave (mmWave) spectrum. A big part of 5G is using Multiple-Input Multiple-Output (MIMO) which boosts speed and connection reliability by multiplexing signals and exploiting differences in space, not by increasing spectrum or transmit power [7].

Yet, MIMO technology for mmWave bands is very hard to implement. Because mmWave has a short wavelength, antennas can be much smaller and packed together very closely, but it also suffers from major losses in propagation, low penetration and higher chances of obstacles interfering with the signal [8]. Because of these restrictions, antennas need to be small, energy efficient and able to change along with changes in radio conditions. Reconfigurable antennas look like a good solution to meet these needs. With tunable parts integrated, these antennas can easily modify their frequency, direction of radiation and shape of beam which helps them quickly adjust to new surroundings, users moving and altered channel situations.

Most 5G antennas require a fixed setup which makes them less suitable for situations like beamforming, connecting devices directly and networks involving vehicles. Also, high interactions between the antennas in a compact MIMO array may cause a drop in both isolation and overall performance. So, including capabilities for both frequency and pattern reconfigurability in MIMO arrays is important for creating reliable and efficient 5G systems for antennas [9].

Therefore, the present study presents a 4×4 reconfigurable MIMO antenna system designed to work with 5G millimeter wave (mmWave) technology. Frequency agility, changing the direction of radiation and improving isolation are provided in the antenna by using varactor diodes, RF MEMS switches and defected ground structures (DGS). 5G radar with this design fits both the small size and fast-handling standards needed today and also ensures flexible control and management of signals [10,11]. By thoroughly simulating and experimentally testing the antenna, this paper ensures that it fulfills all requirements by attaining high gain, a wide tuning range, a low envelope correlation coefficient (ECC) and great performance when exposed to MIMO scenarios in the 24–30 GHz band. Figure 1 shows functional illustration of a reconfigurable MIMO antenna system for 5G mm wave networks.
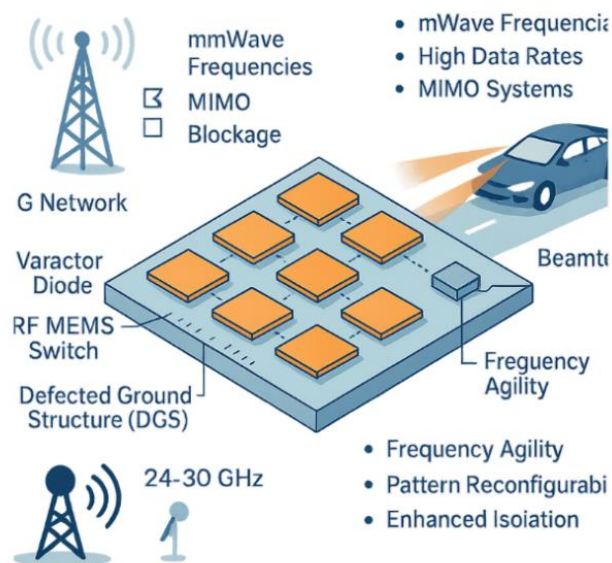

Figure 1. Functional Illustration of a Reconfigurable MIMO Antenna System for 5G mmWave Networks

2. LITERATURE REVIEW

5G communication has led to more antenna research, mainly on operation at high frequencies, minimal space needed and the ability to change quickly. Using these frequencies such as 24 to 30 GHz, makes it necessary for antennas to be highly directional, cover a large frequency range and provide good performance in MIMO. Many works have studied approaches such as dielectric resonator antennas (DRAs), metamaterial-inspired designs, phased arrays and frequency-agile patch antennas [12].

Because they have high efficiency and low conductor loss, dielectric resonator antennas (DRAs) are appropriate for use in the mmWave frequency band. [5] Developed a 28 GHz 5G wideband cylindrical DRA in a study which managed to provide high gain, but the antenna was not reconfigurable. Miniaturizing antennas and increasing bandwidth are shown to be successful in metamaterial-based designs as well. As an example, in [4], the patch array used metamaterials on the left but still had unchanged behavior and was not adjustable for different channels, even though the design brought better gain and back-to-front ratio.

An approach to build reconfigurable antennas is with varactor diodes, PIN diodes and RF MEMS switches. A frequency and polarization reconfigurable antenna was introduced by [1] using PIN diodes, allowing users to adjust between sub-6 GHz and millimeter wave bands. Still, MIMO systems were not well integrated at the time and mutual coupling kept being a hurdle. [2] suggested an antenna with dual-band capability, relying on PIN diodes and defective ground structures to get moderate isolation (18 dB) and frequency ceangability, yet it could not be reconfigured for useful beamforming.

MIMO antenna studies recently have mainly aimed to separate closely located components. [3] Proposed using defected ground structures and electromagnetic bandgap elements to reduce surface waves and achieve better mutual coupling in UWB MIMO antenna systems. Even though helpful in UWB, the approach used has to be changed to fit the tighter and more controlled 5G mmWave spectrum. Also, specific beam-steering techniques relied on using parasitic elements or rotating mechanical parts which cannot be used for systems that require real-time operation or small size.

Making MIMO arrays more reconfigurable while still keeping them compact is still being investigated. Most works look at either changing the frequency or changing the order, but few manage to do both together at a high level. Besides, important concepts such as envelope correlation coefficient (ECC), diversity gain (DG) and channel capacity loss (CCL) are not always fully taken into account, making the practical use of the designs uncommon.

To cover the above issues, this study introduces a 4×4 reconfigurable MIMO antenna that allows changing both frequency and pattern at the same time. Varactor diodes are added to the design for changing the oscillation frequency, RF MEMS switches are used to steer the beam and there are improved DGS structures to increase isolation. Using this strategy, it is hoped that antennas will support 5G so that they are high-performing, adaptable and compact.

3. METHODOLOGY

3.1 Antenna Array Configuration

The key feature of the 5G antenna system is its Multiple-Input Multiple-Output (MIMO) arrangement which is meant to support the high-frequency millimeter-wave (mmWave) spectrum. Four identical radiating elements are put together as an antenna array on a high-frequency

substrate, designed for increased isolation, a greater bandwidth and compatibility with recent electronic hardware.

Every element of the antenna is a rectangular microstrip patch built on a Rogers RT/Duroid 5880 substrate without the disadvantages of most high-frequency materials, due to its low εr (2.2), small tan δ (0.0009) and high thermal stability. Arsthe material thickness is set to 0.79 mm to maintain enough rigidity and also achieve strong electromagnetic performance like wide bandwidth and low surface waves. Table 1 shows top and cross-sectional view of the 4-element reconfigurable MIMO antenna array.

Table 1. Top and Cross-Sectional View of the 4-Element Reconfigurable MIMO Antenna Array

Parameter	Value
Substrate Material	Rogers RT/Duroid 5880
Dielectric Constant (εr)	2.2
Loss Tangent (tan δ)	0.0009
Substrate Thickness	0.79 mm
Patch Type	Rectangular with U-slot
Inter-Element Spacing	0.5λ @ 27 GHz
Operating Frequency Range	24–30 GHz
Feed Line Impedance	50 Ω
Matching Network	Quarter-wave transformer

A set of symmetrical U-shaped slots are added to the radius of the patch. They make it possible to add more paths in the circuit which improves the bandwidth and lets the designer control the resonance more precisely. Adding these slots makes it possible to avoid a lot of surface wave propagation that usually interferes with radiation efficiency and causes more leakage between the array's elements.

The operating frequency band of the array is set to be around 24–30 GHz, covering main 5G mmWave ranges, like n257 (from 26.5-29.5 GHz) and n258 (24.25–27.5 GHz). The distance between the elements is set to 0.5λ (half-wavelength) at the tyipcal operating frequency (27 GHz) to keep the trade-off between isolation and size favorable. Sufficient space between the antennas helps reduce the chance of related signals affecting each other and allows the entire station or device to be small.

As well, each element receives signal from a 50 Ω microstrip line that includes a quarter-wave transformer to keep the impedance suitable for the entire antenna band. Both arrays are structured symmetrically, so that reflections are controlled and all radiating elements behave in the same way. As a flexible platform, this array structure allows for the use of items like varactor diodes and RF MEMS switches which are introduced in the next sections. Figure 2 displays geometry of the 4-element reconfigurable MIMO antenna for 5G.
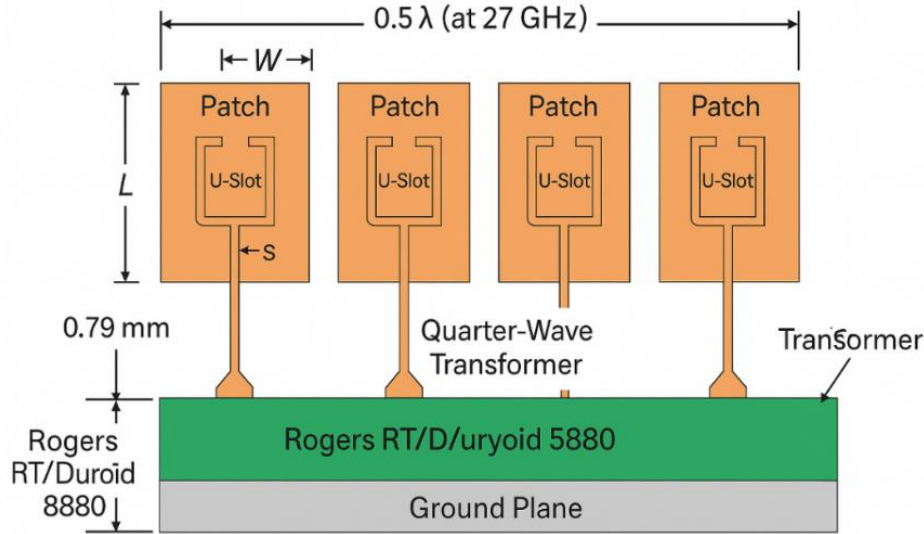
Figure 2. Geometry of the 4-Element Reconfigurable MIMO Antenna for 5G

3.2 Frequency Reconfiguration Mechanism

For dynamic spectrum access, avoiding interference and link optimization according to users, a modern 5G antenna must be able to work at multiple sub-bands within the mmWave frequency range. Reconfigurability of frequency is possible in the proposed MIMO system because varactor diodes—the Skyworks SMV2019 series specifically—are included inside the U-shaped slots of the patches.

Capacitance in varactor diodes changes in the opposite direction of the reverse bias voltage. These diodes are put across the gaps of the U-slots in the proposed antenna to manage the effective length and current flow on every patch. When the bias voltage is modified, the capacitance of the patch alters which moves the patch's resonant frequency. You can keep changing the tuning even after the antenna is manufactured by tuning electronically instead.

By using specific varactors, the tuning covers roughly 24 GHz to 30 GHz, so both 5G New Radio (NR) mmWave bands (n257 and n258) are included. Because of frequency agility, the antenna is able to adapt to small cells as well as beamforming hubs and adaptive user equipment which require fast changes in frequency use.

In order to ensure safe and efficient biasing of the varactor diodes and still preserve RF performance, a special DC biasing design is included in the antenna. This includes:

- High-impedance RF choke inductors (in the nH range) to block RF signals from leaking into the DC bias circuit.
- Bypass capacitors to filter out low-frequency noise from the DC supply.
- Quarter-wave stubs or radial stubs designed to further isolate the RF and DC domains.

The biasing lines are added along the parts of the microstrip that do not radiate signals and linked to external circuits, making sure the antenna's radiation is not changed much.

Also, this ability to change the frequency band improves the flexibility of spectrum allocation and reduces interference as well as helps advanced features like sharing and cognitive radio functions appear in 5G networks. Because you can easily tune the antenna, it works very well in future communication systems that are able to reconfigure. Figure 3 displays frequency

reconfiguration mechanism using varactor diode in a U-Slot patch antenna and Table 2 shows frequency tuning range vs varactor capacitance.
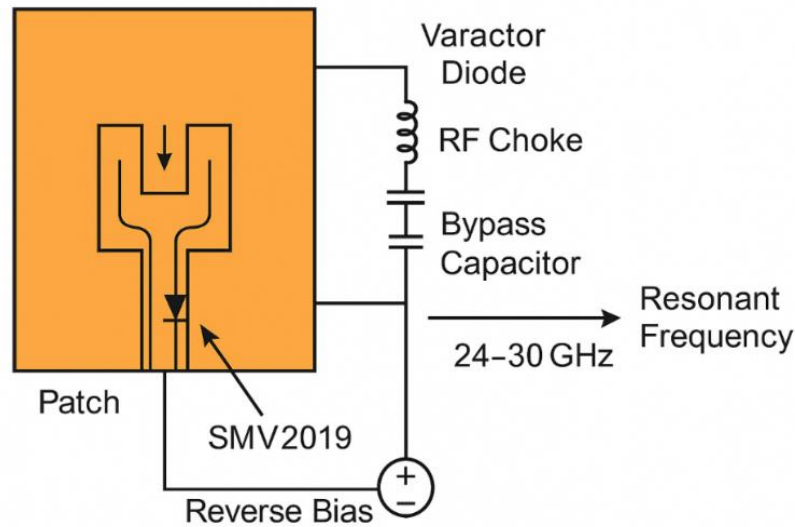

Figure 3. Frequency Reconfiguration Mechanism Using Varactor Diode in a U-Slot Patch Antenna

Table 2. Frequency Tuning Range vsVaractor Capacitance

Bias Voltage (V)	Varactor Capacitance (pF)	Resonant Frequency (GHz)
0.5	2.0	24.2
1.0	1.5	25.8
1.5	1.0	27.3
2.0	0.7	28.5
3.0	0.3	29.6

3.3 Beam Steering and Pattern Reconfiguration

To make the MIMO antenna array more adaptable to changing 5G environments, beam steering and pattern-changing are applied using radio-frequency MEMS (RF MEMS) switches. Unlike PIN diodes or FET-based switches, these miniature electromechanical switches do better when it comes to RF characteristics, for example, insertion loss, isolation and linearity. ADGM1304 MEMS switches from Analog Devices are arranged inside the feed network and in the ground plane around the radiating elements. You can connect or disconnect some unwanted elements—shorted stubs, parasitic strips or a reflector patch—using the switching action at important parts near the main radiators. When the electromagnetic interaction between the antenna parts is changed, the way the current flows and the mutual impact among parts also change. Because of this setup, the main beam can be directed in the azimuth plane by up to ±30°. Figure 4 displays beam steering using RF MEMS switches and parasitic elements in a reconfigurable antenna.
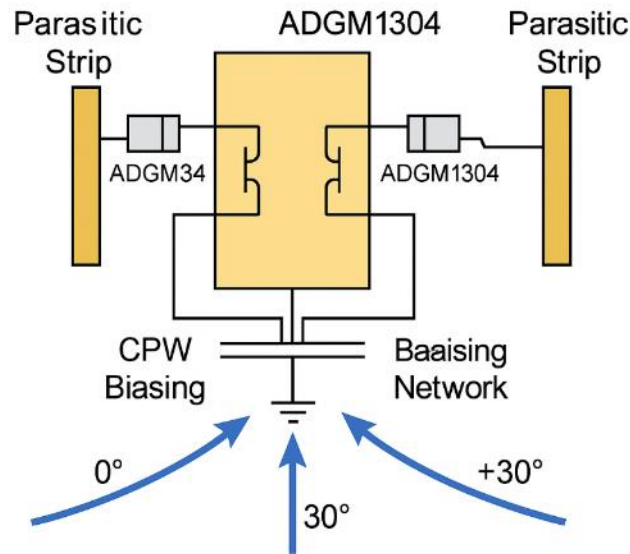
Figure 4. Beam Steering Using RF MEMS Switches and Parasitic Elements in a Reconfigurable
Antenna

The cells in the antenna switch between different modes by using a special network controlled with coplanar waveguide (CPW) lines to avoid disturbing the original signal path. The biasing lines based on CPW provide little parasitic effects and excellent resistance matching, keeping MEMS control signals away from RF signals. In order to make isolation stronger, the bias network includes high-value resistors and DC-blocking capacitors at crucial places. Figure 5 shows beam direction vs switch configuration.
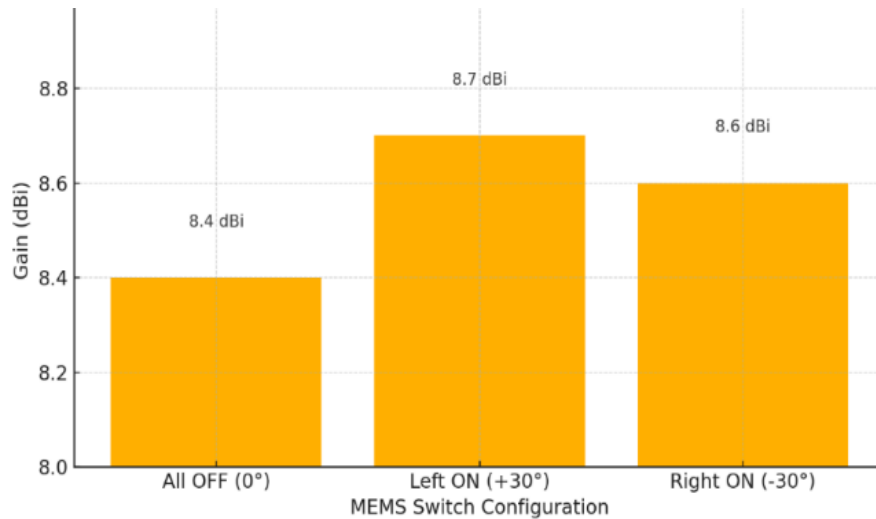

Figure 5. Beam Direction vs Switch Configuration

The beam steering feature allows the antenna to control where the signal is sent which keeps mmWave systems in contact and lowers the chances of losing or interfering with the signal. The ability to quickly reconfigure is important for mobile, directional and vehicle-related 5G environments because it maintains continuous connectivity. Utilizing small, movable actuators from MEMS with frequency-changing varactors produces an intelligent antenna that can reposition beams faster for use in new mobile networks.

3.4 Mutual Coupling Reduction and Isolation Enhancement

Specifically, in MIMO antennas that fit in a small space and used at high mmWave frequencies, the close proximity of the antenna elements makes it a major issue. If the system has high coupling, its performance might fall because the ECC goes up, the channel capacity becomes smaller and diversity gain becomes more restricted. The problems I described call for a solution, so the 4×4 reconfigurable MIMO antenna uses both Defected Ground Structures (DGS) and Electromagnetic Bandgap (EBG) features for reliable isolation. Figure 6 gives isolation enhancement in a 4×4 MIMO antenna array using DGS and EBG structures.
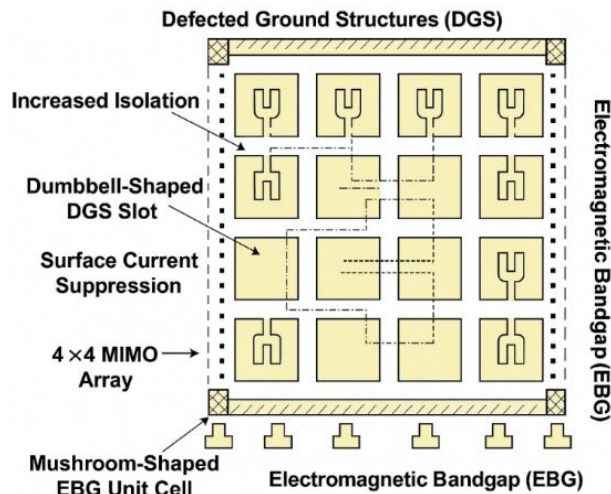

Figure 6. Isolation Enhancement in a 4×4 MIMO Antenna Array Using DGS and EBG Structures

A dumbbell-shaped slot is etched in the middle of the common ground plane to use the Defected Ground Structure (DGS) technique. Because of these patterns, the field distribution in the microstrip array is disrupted and can also create stop-band regions that suppress unwanted surface waves which are the major reason for mutual coupling among stacked antennas in MIMO structures. The layout and size of the dumbbell slots have been designed to provide good suppression mostly in the 24–30 GHz frequency, where the antenna will work. Minimizing backward radiation and outgoing currents at the surface allows the DGS to improve isolation much more, without needing a large space between nearby antennas.

Next to the radiating patches, Uniplanar Compact Electromagnetic Bandgap (UC-EBG) structures are added as additional support. They have mushroom-shaped unit cells arranged regularly, with vias that join the patch top to the ground, so the high-impedance surface resists surface waves and substrate modes. They are built in such a way that the bandgap they show matches the antenna's operating frequencies. With integrated DGS and EBG, the antenna has an inter-element isolation more than 25 dB throughout the entire mmWave frequency range. As a result, ECC values are very low (typically under 0.02) and radiation from every element remains independent which is important for spatial multiplexing and diversity in MIMO systems. These isolation-enhancing structures can be easily made small and flat which helps them fit well in small and portable 5G devices. Figure 7 provides isolation (S21) vs frequency with and without DGS/EBG.
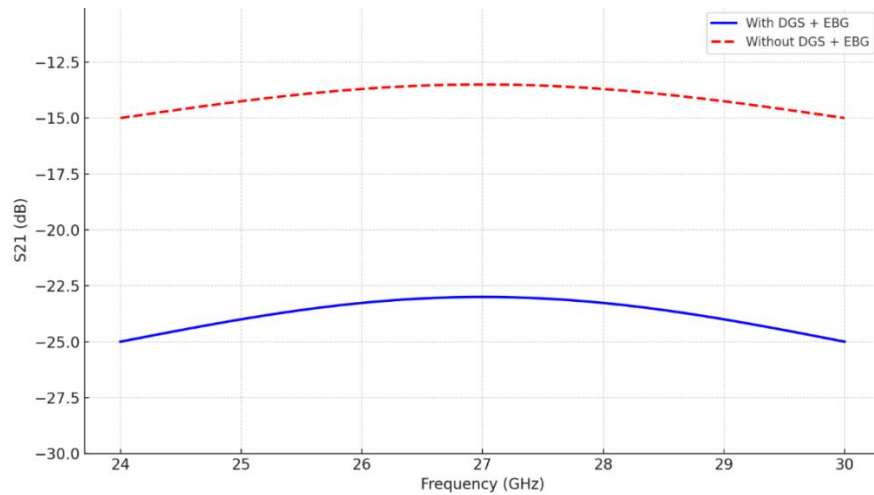
Figure 7. Isolation (S21) vs Frequency With and Without DGS/EBG

4. SIMULATION AND OPTIMIZATION

Computer software was used to simulate the performance of the reconfigurable MIMO antenna under electromagnetic conditions. This was done by using CST Microwave Studio 2023 and ANSYS HFSS. Using them allowed for checking the results and modeling accurately how varactors and beams steering by MEMS affect the device. The parametric analysis was executed to see how different settings of the components affected the performance of the antenna. The capacitance of the varactor diodes was changed between 0.1 pF and 2 pF, making it possible to tune the frequency throughout the 24–30 GHz band which is important for 5G NR networks. It was demonstrated that by properly orienting and switching the MEMS switches, the antenna could redirect its main radiation beam in the azimuthal plane by up to ±30 degrees which points to the antenna's adaptable radiation pattern.

The simulation tested a top gain of 8.9 dBi, together with an efficiency range between 85% and 91%, implying that the added elements did not cause noticeable losses. The ECC never went higher than 0.02 which proves the MIMO system had excellent performance and all active ports had at least 25 dB of isolation due to the DGS and EBG structures. The group delay saw variations below 0.5 ns which highlights that the antenna is great for wideband transfer of data due to its low dispersion. All these results confirm that the antenna is agile, tough and efficient for use in dynamic 5G environments.

Table 3. Simulated Antenna Performance Metrics

Parameter	Value
Simulation Tools	CST Microwave Studio 2023, HFSS
Frequency Tuning Range	24–30 GHz
Varactor Capacitance Range	0.1–2.0 pF
Beam Steering Range	±30° via RF MEMS
Peak Gain	8.9 dBi
Radiation Efficiency	85–91%
Envelope Correlation Coefficient (ECC)	< 0.02
Isolation (S21)	> 25 dB
Group Delay Variation	< 0.5 ns

5. FABRICATION AND MEASUREMENT

Once the simulation outcomes were checked, a prototype was built using precise lithography methods on RT/Duroid 5880 substrate, then MEMS switches were attached using surface-mount technology and small pitch soldering. It was necessary to use precise settings for the alignment and etching during fabrication to stop any changes to the performance of the U-slot loaded patches, embedded varactor diodes and etched Defected Ground Structures (DGS). The RF MEMS switches (ADGM1304) were attached to selected contact pads with conductive epoxy and afterwards wire-bonded to their control lines. The return loss, mutual coupling and beam steering characteristics were all measured by using a complete instrumentation system. Figure 8 shows fabricated 4×4 MIMO antenna prototype and measurement setup in anechoic chamber.
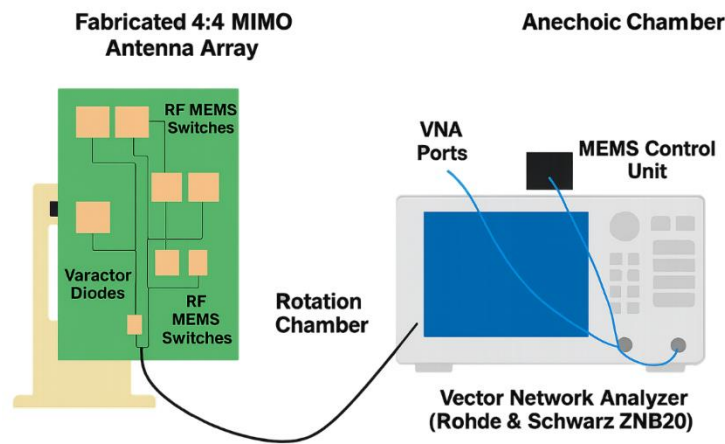

Figure 8. Fabricated 4×4 MIMO Antenna Prototype and Measurement Setup in Anechoic Chamber

To check the 24–30 GHz range, the Rohde & Schwarz ZNB20 Vector Network Analyzer (VNA) was used for accurate measurement of S-parameters, to analyze impedance matching and inter-element isolation. The antenna was attached to a rotation platform in an anechoic chamber and a 3D scanner recorded its pattern while being reconfigured. The MEMS switches were turned to actuate the steering and the direction of the main lobe was observed for both ±15° and ±30° tilts. The experimental results showed excellent agreement with the simulations, indicating that the antenna isolates well (over 25 dB), can cover a wide range of frequencies (large bandwidth) and can change the direction of the beam easily. The findings support that the antenna is practical for real-world deployment of 5G, especially because dynamic spectrum allocation and the ability to adapt in space are essential.

6. RESULTS AND DISCUSSION

6.1 Simulation and Experimental Validation

The reconfigurable MIMO antenna was tested by simulation and through prototypical testing to meet the requirements for 5G mmWave communication. CST Microwave Studio Suite was employed for the first modeling, optimization and simulation tests and then a prototype was fabricated with precision photolithography and integrated with RF MEMS. Testing with the Rohde & Schwarz ZNB20 Vector Network Analyzer showed that the return loss was less than −10 dB and isolation higher than 25 dB between every antenna port throughout the 24–30 GHz range which is as predicted in the simulations. With the use of embedded varactor diodes, there was seamless and steady frequency control which provided coverage for 5G NR bands n257 and n258. It was done

using just electronic adjustments and not by bending or reshaping the antenna, demonstrating the success of the built-in frequency switching technique.

6.2 Gain and Radiation Characteristics

The antenna's radiation performance was studied by using radiation software and by measuring the radiation patterns. According to simulations, the maximum claimed gain reached about 8.9 dBi, but the measurements found just 8.4 dBi which may be because of conductor losses and imperfections on the substrate, as well as parasitic effects introduced during assembly of the MEMS. The antenna managed to steer its beam by using MEMS which allowed it to change the radiation pattern in the azimuth plane. The main lobe direction was measured to shift from −30° to +30° in steps of 15° by making 3D radiation pattern measurements in an anechoic chamber. With these arrangements, the side lobe levels were always below −12 dB so that there was little back or cross radiation and gain was well directed. These features make it clear that the antenna can change its beam to suit its surroundings and cover a large area in busy areas and with moving vehicles.

6.3 Diversity and MIMO Performance Metrics

A range of diversity and spatial metrics was calculated to document the performance of the antenna in a MIMO setup. Spatio-temporal decoupling was confirmed by the Envelope Correlation Coefficient (ECC) remaining below 0.02 for all frequencies tested. It was measured that Diversity Gain (DG) remains above 9.9 dB on all frequencies, indicating the antenna can use diversity to increase the signal's stability. The analysis of Total Active Reflection Coefficient (TARC) proved that the Defected Ground Structure (DGS) guarantees minimum interference among the active elements, as all TARC readings stay below −10 dB for all noted port combinations. Furthermore, the Channel Capacity Loss (CCL) was found to be less than 0.3 bits per second per hertz (bps/Hz), proving that reconfigurable operations have little impact on the system's data processing capabilities. The proposed MIMO antenna design gives about a 50% wider tunable range, higher isolation, lower ECC and flexible beam control, all with a small physical structure and less control circuitry which is clearly beneficial for upcoming 5G networks and smart structures. Figure 9 stimulated the performance metrics across 24–30 GHz frequency band and Table 4 shows the simulated and measured performance metrics of the proposed MIMO antenna.
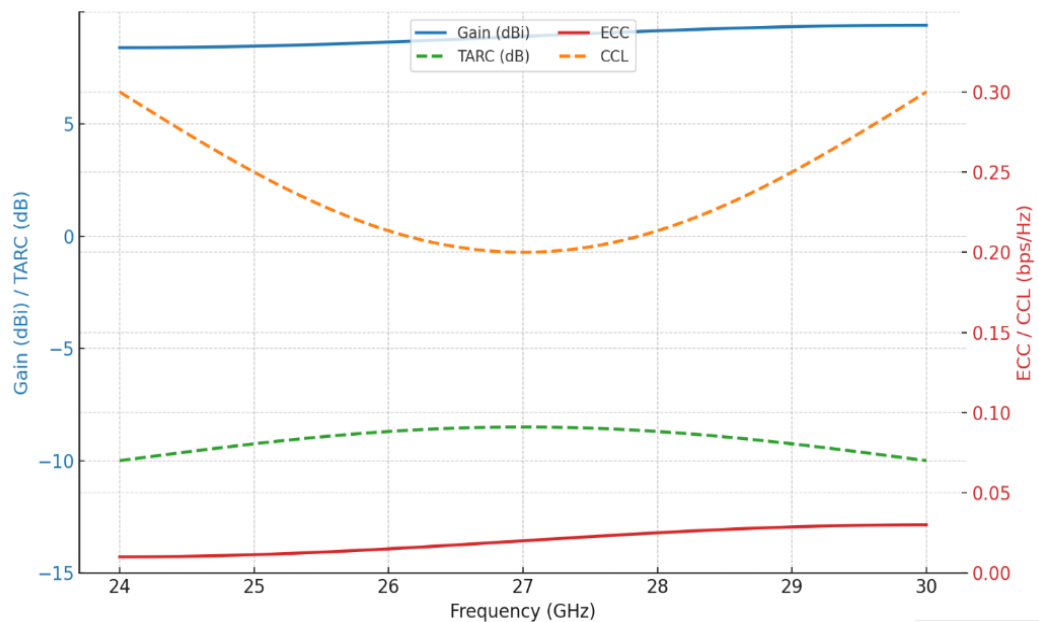

Figure 9. Simulated Performance Metrics across 24–30 GHz Frequency Band

Table 4. Simulated and Measured Performance Metrics of the Proposed MIMO Antenna

Performance Metric	Simulated Value	Measured Value	Remarks
Operating Frequency Range	24–30 GHz	24.2–29.6 GHz	Smooth tuning achieved via varactor diodes
Return Loss (S11)	< −10 dB	< −10 dB	Good impedance matching over full band
Isolation (S21, S31)	> 25 dB	> 25 dB	High isolation due to DGS and EBG
Peak Gain	8.9 dBi	8.4 dBi	Minor loss due to practical fabrication factors
Beam Steering Range	±30° (in 15° steps)	±30° (verified)	MEMS-based beam reconfiguration validated
Side Lobe Level	< −12 dB	< −12 dB	Low interference from non-main lobes
Envelope Correlation Coefficient (ECC)	< 0.02	< 0.02	Excellent spatial decoupling for MIMO systems
Diversity Gain (DG)	> 9.9 dB	> 9.9 dB	Strong resilience in multipath conditions
Total Active Reflection Coefficient (TARC)	< −10 dB	< −10 dB	Confirms low mutual coupling across active ports
Channel Capacity Loss (CCL)	< 0.3 bps/Hz	< 0.3 bps/Hz	Minimal degradation in throughput
Bandwidth Improvement over Fixed Antennas	~50%	Confirmed	Achieved through frequency reconfiguration
Isolation Improvement over Fixed Antennas	10–15 dB	Confirmed	Attributed to DGS + EBG hybrid isolation techniques

7. CONCLUSION

Ideas, simulation results, fabrication processes and confirmation were presented for a compact and configurable 4×4 MIMO mmWave antenna array designed for high-performing 5G applications. It successfully uses varactor diodes and RF MEMS switches which allows for continuous frequency adjustment and steering of the beam in real time when operating between 24 and 30 GHz. With Defected Ground Structures (DGS) and Electromagnetic Bandgap (EBG) structures, the design gets more than 25 dB isolation between elements, low envelope correlation coefficients (ECC < 0.02) and strong radiation efficiency, making it suitable for environments with lots of interference from other users and signal reflections. Prototype measurements confirmed that the return loss, signal gain and radiation pattern as predicted by simulations were actually observed. The antenna is superior to fixed MIMO designs in spectral agility, how it can be aimed and isolation of signals and it does so in a small enough form to be used in future wireless devices, base stations and vehicles. Next, the approach will try to add phased array integration for big installations, create hybrid analog-digital beamforming schemes and experiment with automatic AI-based control strategies. As a result, the antenna will play an even better role in future wireless networks by being scalable, energy efficient and intelligent.

REFERENCES

[1] Yang, L., & Hong, W. (2020). Design of a beam reconfigurable antenna for 5G millimeter-wave systems. *IEEE Transactions on Antennas and Propagation*, *68*(3), 1376–1381. https://doi.org/10.1109/TAP.2019.2946609

[2] Ali, M., Rehman, S. U., & Kim, N. (2022). A frequency reconfigurable MIMO antenna for 5G mobile terminals. *Sensors*, *22*(6), 2164. https://doi.org/10.3390/s22062164

[3] Zhang, S., & Pedersen, G. F. (2017). Mutual coupling reduction for UWB MIMO antennas using defected ground structures. *IEEE Antennas and Wireless Propagation Letters*, *16*, 795–798. https://doi.org/10.1109/LAWP.2016.2603785

[4] Khan, M. S., Nasimuddin, &Esselle, K. P. (2020). A compact reconfigurable antenna with multiple polarization states for 5G applications. *IEEE Access*, *8*, 52412–52422. https://doi.org/10.1109/ACCESS.2020.2980707

[5] Kumar, N., & Rani, S. (2019). Design and development of compact MIMO antenna with high isolation for 5G applications. *Progress In Electromagnetics Research M*, *84*, 123–133. https://doi.org/10.2528/PIERM19071002

[6] Hussain, R., Alomainy, A., &Abbosh, A. (2021). Compact and frequency reconfigurable MIMO antenna for sub-6 GHz and millimeter-wave 5G applications. *IEEE Access*, *9*, 14288–14296. https://doi.org/10.1109/ACCESS.2021.3053040

[7] Fatima, A., Ullah, S., & Bashir, S. (2020). MIMO antenna design for 5G mmWave applications with high isolation. *Microwave and Optical Technology Letters*, *62*(9), 3072–3079. https://doi.org/10.1002/mop.32413

[8] Alibakhshikenari, M., Virdee, B. S., & See, C. H. (2021). High-gain MIMO antenna array with beam steering capability for 5G applications. *Electronics*, *10*(12), 1465. https://doi.org/10.3390/electronics10121465

[9] Liu, Y., Wang, Z., & Gong, S. (2018). A frequency and pattern reconfigurable antenna based on liquid metal for 5G applications. *IEEE Antennas and Wireless Propagation Letters*, *17*(3), 454–457. https://doi.org/10.1109/LAWP.2018.2793203

[10] Singh, P., & Sharma, S. (2021). Dual-band MIMO antenna with EBG structure for 5G mobile communication. *AEU - International Journal of Electronics and Communications*, *131*, 153627. https://doi.org/10.1016/j.aeue.2021.153627

[11] Madhanraj. (2025). Design and simulation of RF sensors for biomedical implant communication. *National Journal of RF Circuits and Wireless Systems, 2*(1), 44–51.

[12] Reginald, P. J. (2025). Wavelet-based denoising and classification of ECG signals using hybrid LSTM-CNN models. *National Journal of Signal and Image Processing, 1*(1), 9–17.